

Neutrophil-Bead Collision Assay: Pharmacologically Induced Changes in Membrane Mechanics Regulate the PSGL-1/P-Selectin Adhesion Lifetime

K. E. Edmondson,^{*†} W. S. Denney,^{*‡} and S. L. Diamond^{*†‡}

^{*}Institute for Medicine and Engineering, [†]Department of Bioengineering, and [‡]Department of Chemical and Biomolecular Engineering, University of Pennsylvania, Philadelphia, Pennsylvania

ABSTRACT Visualization of flowing neutrophils colliding with adherent 1- μm -diameter beads presenting P-selectin allowed the simultaneous measurement of collision efficiency (ϵ), membrane tethering fraction (f), membrane tether growth dynamics, and PSGL-1/P-selectin binding lifetime. For 1391 collisions analyzed over venous wall shear rates from 25 to 200 s^{-1} , ϵ decreased from 0.17 to 0.004, whereas f increased from 0.15 to 0.70, and the average projected membrane tether length, L_{tether}^m , increased from 0.35 μm to ~ 2.0 μm over this shear range. At all shear rates tested, adhesive collisions lacking membrane tethers had average bond lifetimes less than those observed for collisions with tethers. For adhesive collisions that failed to form membrane tethers, the regressed Bell parameters (consistent with single bond Monte Carlo simulation) were zero-stress off-rate, $k_{\text{off}}(0) = 0.56 \text{ s}^{-1}$ and reactive compliance, $r = 0.10 \text{ nm}$, similar to published atomic force microscopy (AFM) measurements. For all adhesion events (\pm tethers), the bond lifetime distributions were more similar to those obtained by rolling assay and best simulated by Monte Carlo with the above Bell parameters and an average of 1.48 bonds ($n = 1$ bond (67%), $n = 2$ (22%), and $n = 3\text{--}5$ (11%)). For collisions at 100 s^{-1} , pretreatment of neutrophils with actin depolymerizing agents, latrunculin or cytochalasin D, had no effect on ϵ , but increased L_{tether}^m by 1.74- or 2.65-fold and prolonged the average tether lifetime by 1.41- or 1.65-fold, respectively. Jasplakinolide, an actin polymerizing agent known to cause blebbing, yielded results similar to the depolymerizing agents. Conversely, cholesterol-depletion with methyl- β -cyclodextrin or formaldehyde fixation had no effect on ϵ , but reduced L_{tether}^m by 66% or 97% and reduced the average tether lifetime by 30% or 42%, respectively. The neutrophil-bead collision assay combines advantages of atomic force microscopy (small contact zone), aggregometry (discrete interactions), micropipette manipulation (tether visualization), and rolling assays (physiologic flow loading). Membrane tether growth can be enhanced or reduced pharmacologically with consequent effects on PSGL-1/P-selectin lifetimes.

INTRODUCTION

Neutrophils, platelets, and endothelium interact through various bonding mechanisms during inflammation and thrombosis. P-selectin, a dimer presented on activated platelets or activated endothelium, helps to capture flowing neutrophils via P-selectin glycoprotein ligand-1 (PSGL-1) located on neutrophil microvilli. Under flow conditions, the adhesive function of P-selectin/PSGL-1 bonding depends on the sum of discrete chemical interactions in the bond interface as well as the dynamics of macroscopic force transmission to the molecular level via the deformable microvilli. Cellular processes such as membrane tether formation and whole cell deformation affect selectin bond rupture by altering force transmission.

The Bell model is an empirically useful approach for quantifying the force sensitivity of bond lifetimes where $k_{\text{off}} = k_{\text{off}}(0) \exp(rF_B/k_B T)$ and k_{off} is the dissociation constant; F_B is the force on the bond; $k_{\text{off}}(0)$ and r are the experimentally determined unstressed off-rate and reactive compliance, respectively; k_B is the Boltzmann constant; and T is the temperature. Bell model parameters have been measured for selectin-ligand pairs in a variety of ways, including rolling cells and/or rolling beads (1–5); atomic force microscopy (AFM (6–8)); molecular force probe (9,10); laser trap (11); and dynamic force spectroscopy (DFS (12–14)). Values of

$k_{\text{off}}(0)$ determined by extrapolation to zero force for PSGL-1/P-selectin are consistent with those obtained in solution phase using plasmon resonance (15). These different mechanical methods create various force loading profiles to drive bond rupture dynamics (16). At venous wall shear rates of 25–200 s^{-1} , physiological loading during neutrophil capture is characterized by rapid loading ($\sim 1\text{--}50$ ms) to a peak value (~ 10 pN to 100s pN) with subsequent force relaxation due to tether pulling (17–19). Experimental challenges include whether only single bond interactions are being evaluated (20), the requirement of estimating forces and geometries on both microscopic and macroscopic length scales, the integrity of purified molecule presentation, and the temporal/spatial resolution of each method. In general, the $k_{\text{off}}(0)$ of L-selectin is considered to be greater than that of P-selectin or E-selectin, consistent with the fact that neutrophils roll on L-selectin at a velocity 7.5–11.5 times faster than they do on either P or E-selectin (21).

The dimeric PSGL-1 molecule is located primarily on the microvilli tips of neutrophils. Microvilli extend $\sim 0.25\text{--}0.35$ μm from the neutrophil surface as measured by electron microscopy or micropipette aspiration (17), and as calculated based upon comparison of the off-rates of fixed cells and beads (3). Micropipette aspiration techniques have been developed to explore the mechanics of tether formation from neutrophils (17,22,23) and from endothelial cells (24).

Submitted May 10, 2005, and accepted for publication August 3, 2005.

Address reprint requests to S. L. Diamond, Tel.: 215-573-5702; E-mail: sld@seas.upenn.edu.

© 2005 by the Biophysical Society

0006-3495/05/11/3603/12 \$2.00

doi: 10.1529/biophysj.105.066134

Membrane tether formation using micropipette manipulation has revealed two regimes of tether growth: microvilli extension, characterized by linear elastic deformation of the neutrophil ($F_B < 34$ pN); and membrane tether formation, in which lipid membrane flows freely and at a constant velocity when F_B is $> \sim 45\text{--}61$ pN (17,19,22). Between 34 and 61 pN, the formation of a membrane tether versus an extended microvillus depends upon the degree of interaction between cytoskeleton and membrane (17). Membrane tether pulling during flow perfusion over adherent platelets or selectin-coated surfaces is visualized as translation of the cell downstream of an adhesion point at a constant velocity well below that of the free-stream velocity (18).

Pharmacological agents targeting actin polymerization can be used to study the relationship between the cytoskeleton function and cell mechanics. Actin polymerization and membrane fluidity in the leukocyte can be altered using actin-polymerizing agents such as jasplakinolide or depolymerizing agents such as cytochalasins or latrunculin (25–27). Cytochalasins depolymerize actin, although their modes of action and specificity are varied (26). Latrunculin A is a more specific actin depolymerizing agent that binds to actin monomer and prevents incorporation into F-actin. Jasplakinolide increases actin polymerization and stabilization by decreasing the amount of sequestered actin and enhancing F-actin nucleation (28–29) with some observed cytotoxicity (30). Neutrophils treated with cytochalasin B or D exhibit a decrease in cortical tension and cytoplasmic viscosity during aspiration into micropipettes (31–33) or tether extraction by micropipette (23). Similar increases in deformability after treatment with cytochalasin B were also observed in eosinophils (27). Perfusion of neutrophils treated with cytochalasin is associated with localization of PSGL-1 to the pointed ends of teardrop-shaped cells (34). Actin depolymerization is also associated with a loss of membrane ruffles, as evidenced by 1), the ability of cytochalasin B to abolish tether formation (35); and 2), the smooth shape of latrunculin A-treated neutrophils under scanning electron microscope (SEM) (36). In contrast, jasplakinolide treatment of neutrophils results in an increase in global rigidity as measured by aspiration into a micropipette (37). However, AFM elasticity studies of jasplakinolide, cytochalasin, or latrunculin-treated neutrophils suggests that all three reagents reduced the local Young's modulus of the plasmalemma, possibly due to the effect that jasplakinolide caused disaggregation but not disassembly of the actin fibers (38). Also, jasplakinolide can cause membrane blebbing (37). In contrast, the membrane cholesterol content of a cell can also be manipulated to study the effects of membrane fluidity on cell adhesion. Methyl- β -cyclodextrin (M β CD) can be used alone or in complexes with cholesterol to deplete or enrich the plasmalemma with cholesterol, respectively (39). Cholesterol depletion in neutrophils has been shown to be associated with resistance to deformation during aspiration (33), as does chemical fixation. Unexpectedly, M β CD has been reported to reduce neutrophil actin polymerization (40).

To study the effect of neutrophil membrane tether formation on selectin bond mechanics, we developed a new method of probing interactions between a flowing cell and a small point source of ligand presented on a 1- μ m-diameter adherent bead. The advantages of this approach:

1. Discrete reactions can be probed that have a defined initiation time.
2. The small bead perturbs the laminar flow field to a minimal extent, but provides excellent ligand presentation for bonding analogous to the raised platelet pseudo-nucleus or the endothelial nucleus.
3. Adhesion contact area is exceedingly small, and minimizes bonding to a single tether.
4. Both on-processes (i.e., the collision efficiency) and off-processes (i.e., bond lifetime) are probed simultaneously.
5. There is minimal interference of cell body bonding with the surface of the flow chamber.
6. Physiologically relevant force-loading dynamics are created by hydrodynamic flow.
7. High temporal and spatial resolution allows detection and analysis of membrane tether and bond dynamics.

EXPERIMENTAL PROCEDURES

Materials and neutrophil isolation

Human serum albumin (HSA; Golden West Biologicals, Temecula, CA) and fibrinogen (Enzyme Research Labs, South Bend, IN) were stored according to manufacturers' instructions. Polystyrene, 1.05- μ m-diameter microspheres coated with Protein A were obtained from Bangs Labs (Fishers, IN). Labeling the beads with P-selectin was accomplished through the use of a recombinant human P-selectin/Fc chimera (R&D Systems, Minneapolis, MN) where the Fc region is that of human IgG₁. Jasplakinolide, cytochalasin D, and methyl- β -cyclodextrin (M β CD) were purchased from Sigma-Aldrich (St. Louis, MO). Latrunculin A was from R&D Systems and was a kind gift from Dr. P. Janmey (University of Pennsylvania). A monoclonal antibody against human P-Selectin glycoprotein ligand-1 (R&D Systems) was used in control experiments. Formaldehyde used in neutrophil fixation experiments was obtained from Fisher Scientific (Pittsburgh, PA).

Human blood was obtained via venipuncture from healthy adult donors who had not taken any medications in the prior 10 days. Blood was mixed with anticoagulant sodium citrate (9 parts blood to 1 part citrate). Neutrophils were isolated by centrifugation with a separation medium (Cedarlane Laboratories, Hornby, Ontario) as previously described (18,41). Neutrophils were counted and diluted with a 2% solution of human serum albumin in Hank's Balanced Salt Solution (HBSS; Invitrogen, Carlsbad, CA) with Ca^{2+} to a final concentration of $1\text{--}2 \times 10^6$ cells/ml. In some cases, neutrophils were treated with jasplakinolide (10 μ M), cytochalasin D (15 μ M), latrunculin (0.3 μ M), or M β CD (10 mM) for 30 min at room temperature before perfusion. In the case of treatment with formaldehyde, cells were fixed for 15 min with a 3% formaldehyde solution. The cells were then washed and resuspended in HBSS with Ca^{2+} and 2% HSA.

Neutrophil-bead collision assay

Microspheres coated with Protein A were labeled with P-selectin by the method described by Rodgers, et al. (42). Beads were incubated with periodic vortexing for 45 min at room temperature with up to 0.2 μ g/ml P-selectin-IgG chimera. This yielded a Protein A-saturated surface density of $\sim 5.4 \times 10^3$ IgG-chimera/ μm^2 . After labeling, the microspheres were then

washed three times with a solution of 1% HSA in HBSS. In preparation for attachment to the chamber, the beads were then incubated for 4 h at 4°C with 200 $\mu\text{g/ml}$ fibrinogen. Rectangular glass capillaries (Vitrocom, Mountain Lakes, NJ) having a cross-section of 0.2×2.0 mm, a length of 7 cm, and a wall thickness of 0.15 mm were used as flow chambers, as described previously (18,41). Chambers were incubated with fibrinogen (100 $\mu\text{g/ml}$) for 120 min at room temperature. The microspheres were perfused into the chambers, and the bead-coated chambers were incubated at room temperature overnight in order for the beads to have full adhesion to the capillary surface. Bead-coated flow chamber surfaces were then washed and blocked with HBSS with 2% HSA for 5 min before perfusion studies. Fibrinogen caused no β_2 -integrin mediated adhesion since tests employing anti-PSGL-1, calcium-free buffer, or P-selectin-free beads all resulted in zero detectable adhesion (see Results), and resting neutrophils were used that failed to adhere to the chamber walls even at $\gamma_w = 25 \text{ s}^{-1}$.

Neutrophils were perfused into the chambers using a syringe pump (Harvard Apparatus, Holliston, MA) at various wall shear rates (γ_w) as calculated via the Navier-Stokes equation for laminar flow of a Newtonian fluid: $\gamma_w = 6Q/B^2W$, where Q represents the flow rate (cm^3/s), B is the total plate separation (0.02 cm), and W is the width (0.2 cm). The wall shear stress can be calculated from $\tau_w = (6Q\mu)/(B^2W)$, where μ is the buffer viscosity (0.01 Poise at room temperature). For differential interference contrast microscopy, a Zeiss Axiovert 135 microscope with a $63\times$ (NA 1.40) oil immersion objective lens (Plan Apochromat) was used (Carl Zeiss, Jena, Germany). For high-speed imaging, images were captured using a Motion-Corder Analyzer high-speed digital camera (Eastman Kodak, Rochester, NY) at an imaging rate of 240 frames per second (fps). The images were played back at 5 fps or frame-by-frame to videotape for analysis.

During frame-by-frame analysis, adhesive interactions were identified as those collisions that had a visible pause in neutrophil motion lasting for at least one frame, and had velocities that had decreased below the hydrodynamic velocity (Fig. 1, A–D). An adhesion collision efficiency (ϵ) was calculated from these observations as the number of collisions resulting in an adhesive interaction, divided by the total number of collisions observed. The lifetimes of all adhesive interactions were recorded. These values always greatly exceeded those of simple hydrodynamic collision without bonding. Adhesive neutrophils were defined as tether-forming when they translated in the direction of flow at a velocity below the hydrodynamic stream velocity (18). Membrane tethering fraction (f) was defined as the ratio of tether-forming events to the total number of adhesive interactions. Tether lengths were measured using Scion Image or ImageJ software (National Institutes of Health, Bethesda, MD) from the center of the adhesive bead to the lagging edge of the neutrophil. Approach and release velocities were determined by collecting images of neutrophils as they approached, interacted, and released from a bead at 240 fps.

Estimating force on the P-selectin/PSGL-1 adhesive tether

To estimate the force on the tether between neutrophil PSGL-1 and the bead-bound P-selectin, we performed a force balance (Fig. 1 E) as first described by Shao et al. (17),

$$F_S = F_B \cos \theta, \quad (1)$$

$$F_B \sin \theta \cdot l = F_S R + T_S, \quad (2)$$

where F_S is the shear force on the cell, F_B is the force on the bond, T_S is the torque, and L_{tether}^m is the measured projected tether length between the top of the bead and the tether attachment point on the neutrophil. In the case of multiple bond formation, the force was considered equally shared among the bonds. The length of the lever arm, l , and the angle of attachment θ was calculated. A radius $R = 4.25 \mu\text{m}$ was used for the neutrophil (11,18). For the case of neutrophils that formed adhesive interactions with tethers of a length less than the minimum discernible length of 500 nm (Fig. 1 A), we

estimated the lever arm to be the radius of the cell, R . This approximation yields a maximum error of 24.0% when the cell is considered to be an incompressible sphere, and this error decreases logarithmically as the lever arms increases.

Goldman's equations (43) for the relationship between shear stress and the forces experienced by a flowing sphere as it flows parallel to a plane wall were used to solve for F_S and T_S :

$$F_S = 6\pi\tau_w R h C \quad (3)$$

$$T_S = 4\pi\tau_w R^3 D. \quad (4)$$

In these equations, h refers to the distance from the center of the cell to the chamber surface, or $h = R + \delta$, where δ is the gap distance between the neutrophil and the chamber surface (Fig. 1 E). The values C and D are constants that are determined from the ratio of h/R . Release velocities of adherent neutrophils at 100 s^{-1} were determined from distance versus time plots (Fig. 1 D), and were used to determine the average gap distance between neutrophil and chamber surface, $\delta_{\text{release}} = 0.38 \mu\text{m}$. This gap distance is similar to that of neutrophils releasing from adherent platelets ($0.2\text{--}0.3 \mu\text{m}$; (18)), and yielded values of C and D of 1.64 and 0.95, respectively, based upon data given in Goldman et al. (43). In addition, approach gap distances for the nonadhesive interactions ($\delta = 0.86 \pm 0.24 \mu\text{m}$; $n = 19$ interactions) were similar to those for the adhesive interactions ($\delta = 0.86 \pm 0.29 \mu\text{m}$; $n = 25$) for the portion of interactions observed. Using the measured projected tether length, L_{tether}^m , Eqs. 1–4 were solved for θ and F_B . For neutrophils that formed tethers of the minimum discernible length ($L_{\text{tether}}^m = 0.5 \mu\text{m}$), the angle θ was calculated to be 53.6° .

Kinetic Monte Carlo (MC)

Simulations were performed as previously described (44) using Gillespie's algorithm for stochastic reactions (45). Four possible event types were allowed at a given time-step: 1), breaking a P-selectin/PSGL-1 bond; 2), creating a new bond; 3), growth of the tether; and 4), departure of the neutrophil from the bead after the final bond broke. A bond was defined with respect to the surface densities on a per-protein interface basis such that a total of two bonds could be counted between one PSGL-1 and one P-selectin molecule, since both are dimers. According to the stochastic theory, each of the events has the following probability: 1), $a_1 dt = k_{\text{off}}(F, r) n dt$; 2), $a_2 dt = k_{\text{on}} X_{\text{PSGL-1}} X_{\text{P-selectin}} dt$; 3), $a_3 dt = \bar{v}_t / d_t dt$; and 4), $a_4 dt = \gamma \delta_{n,0} dt$. The contact area ($0.071 \mu\text{m}^2$) was assumed to be a circle with the diameter of the tether ($d_t \sim 300 \text{ nm}$; (46)). We assumed that the initial conditions for the simulations consisted of $n = 1$ or 2 bonds, $X_{\text{PSGL-1}} = 100$ free PSGL-1 and $X_{\text{P-selectin}} = 770$ P-selectins (for ~ 50 PSGL-1 dimers per microvillus (47,48), for $10\text{--}15$ thousand dimers on 252 microvilli per cell (48,49); $\sim 5.4 \times 10^3$ P-selectin chimeras/ μm^2). For each event simulated, the tether growth velocity was randomly selected from the experimental mean tether growth rate (\bar{v}_t) distribution obtained at each wall shear rate (γ). The value $\delta_{n,0}$ is the δ -function and equals 1 when no bonds are present, thus allowing escape of the neutrophil.

Using MC, the values of k_{on} , k_{off} , and r were determined by minimizing the global error between the simulated and measured bond lives at all shear rates. The Bell model was used for determining the off-rate $k_{\text{off}}(F_B, r) = k_{\text{off}}^0 \exp(rF_B / nk_b T)$. The simulated data was compared to experimental data at each shear rate, and the global weighted fitness over all shear rates was evaluated by minimizing

$$f = \sum_{\gamma} \frac{n_{\gamma, \text{ex}}}{N_{\text{tot,ex}}} \frac{|\bar{t}_{\gamma, \text{ex}} - \bar{t}_{\gamma, \text{sim}}|}{\bar{t}_{\gamma, \text{ex}}}, \quad (5)$$

where $n_{\gamma, \text{ex}}$ is the number of experimental data points at a given shear rate; $N_{\text{tot,ex}}$ is the total number of experimental data points; and $\bar{t}_{\gamma, \text{ex}}$ and $\bar{t}_{\gamma, \text{sim}}$ are the experimental and simulated mean times of the adhesion events. For other simulations with a variable number of initial bonds, the bonds were distributed exponentially with up to five bonds initially present via

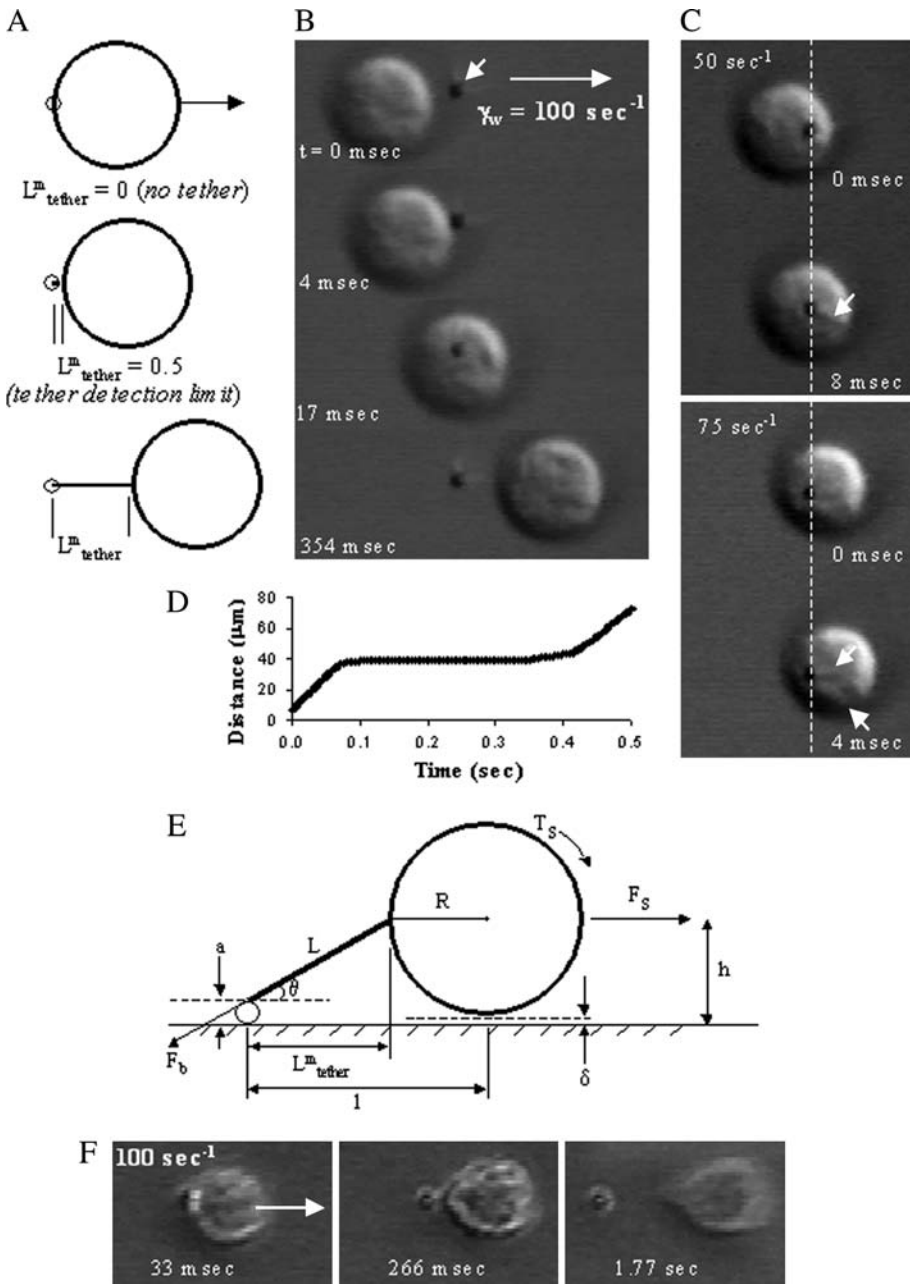


FIGURE 1 Images of neutrophils colliding with and forming tethers on P-selectin-coated beads. The length of tether pulled from the neutrophil is measured from the top of the bead to the lagging edge of the neutrophil (A). This method of measurement imposes a minimum tether length equivalent to the radius of the bead (0.5 μm). A montage of a neutrophil flowing over a bead at $\gamma_w = 100 \text{ s}^{-1}$ is given (B), along with the trajectory of the cell (D). A force diagram is constructed to determine the force on the bond, F_B (E), as described in the text. Small stress lines were detected in the neutrophil membrane, suggesting deformation of the neutrophil. Two representative collisions at $\gamma_w = 50$ and 75 s^{-1} are shown (C), with the stress lines indicated with white arrows. Neutrophil treated with 0.3- μM latrunculin assumed a teardrop-shaped formation under flow (F) as compared to the spherical shape assumed by untreated cells (B).

$$P(n) = \frac{\exp(-dn)}{\sum_{n=1}^5 \exp(-dn)}, \quad (6)$$

where d is the distribution weighting factor.

RESULTS

Adhesion of neutrophils during collision with P-selectin-coated beads

Using 240-fps imaging, we detected the generation of stress lines, or pulling of the ruffles in the membrane of the neutrophil during adhesion to the bead (Fig. 1 C). This rapid

change in morphology represents a direct visualization of the earliest phase of membrane stressing and microvilli extension under flow conditions. Such stress-line features were not present for cells that collided with the bead but failed to form an adhesion to the bead. As the adhesive collision progressed, the formation of membrane tethers began as the neutrophil translated downstream of the bead (Fig. 1 B). Because we were only able to image membrane tethers that grew past a defined minimum discernible length of 0.5 μm (Fig. 1 A), the membrane tether formation that we observed was in the regime of membrane tether formation and not microvillus extension.

We measured the adhesion collision efficiency ε for neutrophil collisions with 1.0- μm P-selectin-coated beads

at various shear rates for three separate donors. The collision efficiency decreased from $\varepsilon = 0.17$ to 0.0043 as γ_w was increased from 25 to 200 s^{-1} (Fig. 2 A). The specificity of bonding interaction was verified at 100 s^{-1} through the use of anti-PSGL-1 monoclonal antibody, adherent beads containing

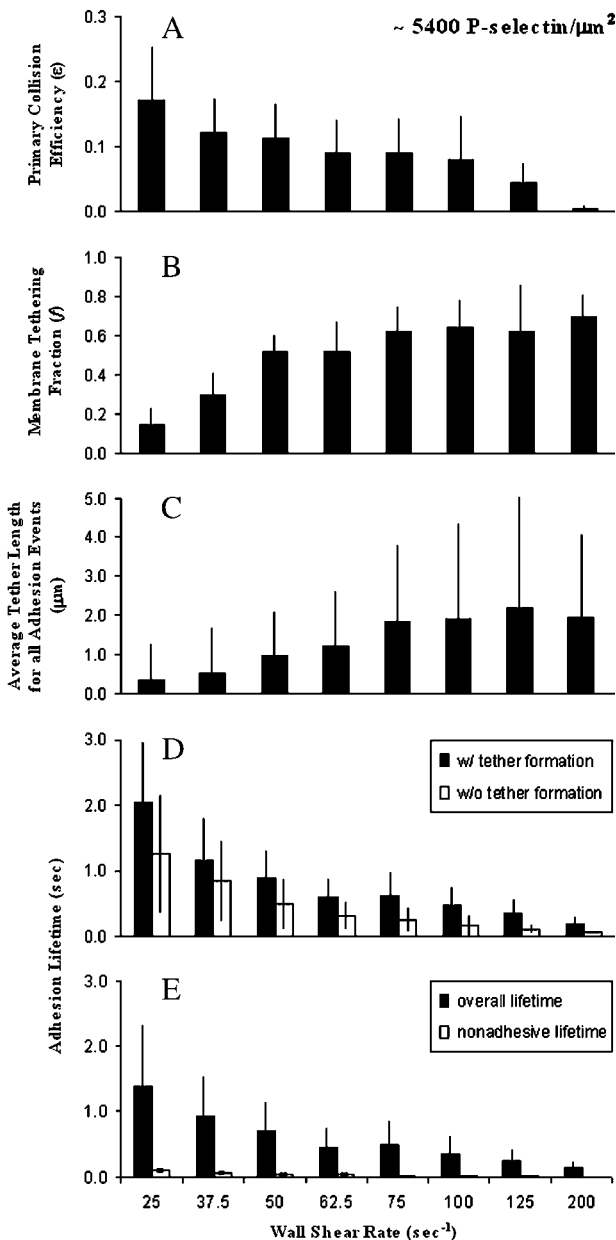


FIGURE 2 Dynamics of neutrophil interaction with P-selectin-coated beads. We calculated the adhesion collision efficiency ε (A) and the membrane tethering fraction f (B) at each shear rate. Error bars for calculated parameters are for $N = 4$ – 10 donors, except in the case at $\gamma_w = 200 \text{ s}^{-1}$, where $N = 2$ donors. Projected tether lengths L_{tether}^m were measured for all neutrophils making adhesive collisions (C). The average lifetimes for all the adhesive and nonadhesive events were calculated (E), and the lifetimes were then binned according to whether they formed discernible membrane tethers (D). Each standard deviation error bar for the measured parameters is for $n > 89$ interactions, and $N = 9$ donors, except in the case of $\gamma_w = 200 \text{ s}^{-1}$, where $n = 20$ interactions.

no P-selectin chimeric IgG, and calcium-free HBSS. In each of these three control cases, no adhesive collisions between neutrophils and beads were observed in over 150 collisions ($\varepsilon = 0$) monitored at each condition (data not shown), compared to $\varepsilon = 0.079$ for P-selectin-coated beads.

The membrane tethering fraction (f), defined as the fraction of adhesive collisions resulting in the formation of an observable membrane tether, was measured at each shear rate (Fig. 2 B). The averages shown in Fig. 2 B were over several donors, with $N > 3$ donors in all cases except at $\gamma_w = 200 \text{ s}^{-1}$, where $N = 2$ due to low capture efficiency ($\varepsilon = 0.0043$). Neutrophils were least likely to form membrane tethers at the lowest shear rates, where membrane tether formation fraction was 0.15 ± 0.08 at $\gamma_w = 25 \text{ s}^{-1}$. The tethering fraction increased to a plateau of ~ 0.62 – 0.70 at $\gamma_w \geq 75 \text{ s}^{-1}$, indicating that neutrophil rolling at venous flows is typically accompanied by tether pulling.

We measured the projected membrane tether length, L_{tether}^m , for each interaction and at each shear rate. For adhesive interactions that formed tethers of length $< 500 \text{ nm}$ (below detection), we assigned a length of $0 \text{ } \mu\text{m}$. For average membrane tether lengths calculated for all adhesive interactions, L_{tether}^m increased from a minimum of $0.35 \pm 0.9 \text{ } \mu\text{m}$ at $\gamma_w = 25 \text{ s}^{-1}$ to a maximum of $\sim 2 \text{ } \mu\text{m}$ at $\gamma_w \geq 75 \text{ s}^{-1}$ (Fig. 2 C), in agreement with prior estimates obtained by reconciling neutrophil and rigid bead pause time distributions (3).

At all shear rates tested, the longevity of binding events that had tethers exceeded the lifetime of events lacking tethers ($p < 0.005$) (Fig. 2 D). We found that the average overall lifetime of adhesion decreased with increasing wall shear rate from $1.38 \pm 0.96 \text{ s}$ at 25 s^{-1} to $0.14 \pm 0.11 \text{ s}$ at 200 s^{-1} (Fig. 2 E). The average lifetime for interactions with and without membrane tether formation exhibited the same trend, decreasing with an increase in wall shear rate (Fig. 2 D). Due to the overall long lifetimes of adhesive bonds at low shear rates, the effect of tether formation at $\gamma_w < 50 \text{ s}^{-1}$ was to increase the overall lifetime of the bond by ~ 1.5 -fold. However, at wall shear rates $\geq 100 \text{ s}^{-1}$, adhesive interactions with membrane tethers experienced lifetimes 3–3.2-fold greater than those without membrane tether formation. These prolongations are consistent with the original predictions of Shao et al. (17). Under all shear conditions, the life of adhesive events greatly exceeded that of nonadhesive hydrodynamic collisions (Fig. 2 E).

From tether lifetime and length data, we calculated a membrane tether growth rate (v_{tether}) for each membrane-tether-forming interaction. These growth rates were averaged at each shear rate tested, and the resultant velocities were plotted as a function of shear rate (Fig. 3). The tether growth rate increased linearly from an average $v_{\text{tether}} = 1.4$ – $21.3 \text{ } \mu\text{m/s}$ over the shear range tested. These results agree with those previously obtained for neutrophil interactions with adherent platelets (18). The critical wall shear rate (x -intercept of Fig. 3) to initiate tether growth was calculated as $\gamma_w = 24 \text{ s}^{-1}$ corresponding to a critical force of $F_{\text{crit}} = 24.3 \text{ pN}$

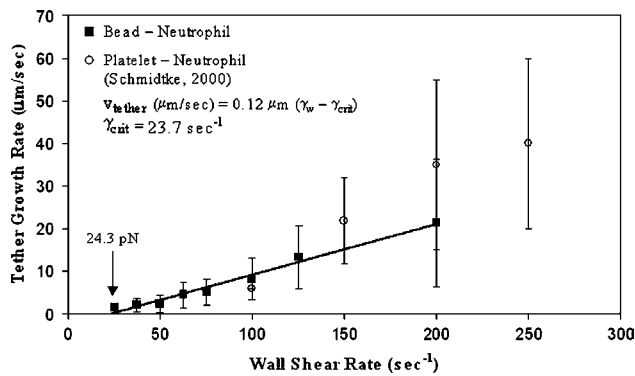


FIGURE 3 Tether growth rates for neutrophils colliding with P-selectin-coated beads. Membrane tether lengths and lifetimes were used to calculate the membrane tether growth rate for untreated cells at $\gamma_w = 25\text{--}200\text{ s}^{-1}$. Our results for neutrophil collision with beads (*solid squares*) were compared with prior results for neutrophils tethering onto platelets (*open circles*; (18)). Error bars are for standard deviation.

($\pm \sim 10\%$), slightly lower than prior measurements made using micromanipulated neutrophils (22,23).

Bell model parameters for PSGL-1/P-selectin

In an effort to characterize the performance of the neutrophil-bead collision assay relative to other assays, we analyzed adhesion lifetime distributions to facilitate the comparison to earlier studies that employed pause-time analysis of flow-chamber rolling data or bond-lifetime distributions from AFM or DFS. To calculate Bell model parameters for the interaction between neutrophils and beads coated with P-selectin, apparent k_{off} values were calculated at each wall shear rate using the average force calculated for the events (using L_{tether}^m for each event). In reality, the set of events collected at each wall shear rate was heterogeneous, since the applied force depends on the length of the tether for each event. For dissociation of the PSGL-1/P-selectin adhesions following first-order kinetics, the decay in number of attached cells was used to graphically fit the apparent kinetic off-rate at each shear rate analyzed (Fig. 4 A), which agreed with the statistical point estimate (SPE) of $k_{\text{off}} = 1/\bar{t}$ (44). Despite the observed variation in tether lengths (and thus force loading) across the events measured at each wall shear rate, the regression plots were highly linear ($R^2 = 0.98$ or 0.99), indicating that linearity is not necessarily proof that a single class of events is being analyzed. The average forces were then used to regress the Bell parameters from values of k_{off} (from the slopes from Fig. 4 A) to obtain the apparent unloaded off-rates and reactive compliance for all data (\pm tethers) (Fig. 4 B) or events lacking tethers (Fig. 4 C). The k_{off} at $\gamma_w = 200\text{ s}^{-1}$ was determined from only 20 events (Fig. 4 B) or eight events (Fig. 4 C) due to the extremely low capture efficiency at this shear rate (approximately four in every 1000 collisions generated an adhesive event). Thus, we also regressed the graph of F_B versus k_{off} with (SPE 2 in Fig.

4, B or C) and without (SPE 1 in Fig. 4, B or C) inclusion of k_{off} at 200 s^{-1} . The weighted Monte Carlo simulation of all shear rates corresponded best with the SPE regression where data at $\gamma_w = 200\text{ s}^{-1}$ was neglected. Cell flattening may also be more pronounced at 200 s^{-1} , thus reducing force loading at this higher level of flow.

We determined the zero-stress off-rate $k_{\text{off}}(0) = 0.67\text{ s}^{-1}$ and reactive compliance, $r = 0.07\text{ nm}$ (Fig. 4 B and curve 1b in Fig. 5 A; $\sim \pm < 8\%$) for all events (\pm tethers) and for $\gamma_w = 25\text{--}125\text{ s}^{-1}$. In comparing these Bell parameters with earlier literature reports (curves 2–14 in Fig. 5), we then evaluated the Bell parameters (by SPE and by MC) for only those events that displayed no detectable membrane tether since the force applied on the adhesion is the same from event to event at a given wall shear rate. These events yielded Bell parameters ($k_{\text{off}}(0) = 0.53\text{ s}^{-1}$, $r = 0.10\text{ nm}$) that 1), were best modeled by single-bond MC (where almost no additional bonds formed); 2), were very poorly fit by a multiple bonding hypothesis ($n = 2$ bonds initially); and 3), were quite consistent with literature values shown in curves 2–8 in Fig. 5 and the recent DFS data of Heinrich et al. (14).

An alternate hypothesis was also tested using the entire data set (\pm tethers) where the MC simulation was performed so that no new bonds could form ($k_{\text{on}} = 0$), assuming that there were no new encounter pairs because of tension on the tether tip continually shrinking the contact area. For $k_{\text{on}} = 0$ and using the Bell parameters obtained for no tether growth ($k_{\text{off}}(0) = 0.53\text{ s}^{-1}$, $r = 0.10\text{ nm}$) as the best estimate of single bond kinetics, we then reanalyzed the entire event set (with and without tethering) and determined that the data set was best fit by a distribution of initial bonds for $d = 1.1$ (Eq. 6) corresponding to an average of 1.48 bonds ($n = 1$ bond, 67%; $n = 2$, 22%; and $n = 3\text{--}5$, 11%; see Appendix for details). We note that the data at $\gamma_w = 200\text{ s}^{-1}$ was quite sparse as a consequence of the extremely low capture efficiency at this shear rate and contributed little to the MC determination of the Bell parameters. Using the Bell parameters obtained for no tether growth and $k_{\text{on}} = 0$, the initial condition of $n = 2$ bonds (a fully engaged dimer interaction) allowed generation of a set of pause times (curve 1c of Fig. 5) quite consistent with the data of Park et al. (3), a result also obtained by King et al. (50). This simulation matched curves 12–14 and was then fit with apparent parameters of $(k_{\text{off}})_{\text{app}} = 0.76\text{ s}^{-1}$ and $r_{\text{app}} = 0.05\text{ nm}$. Figs. 4 and 5 indicate that the neutrophil-bead collision assay allows accurate measurement of lifetime distributions that are consistent with prior measurements and analyses for the PSGL-1/P-selectin interaction.

Chemical treatment of perfused neutrophils

Neutrophils were treated with cytochalasin D (15 μM), latrunculin (0.3 μM), jasplakinolide (10 μM), M β CD (10 mM), or formaldehyde (3% v/v) for 30 min. Latrunculin-treated neutrophils that were perfused at 100 s^{-1} formed an

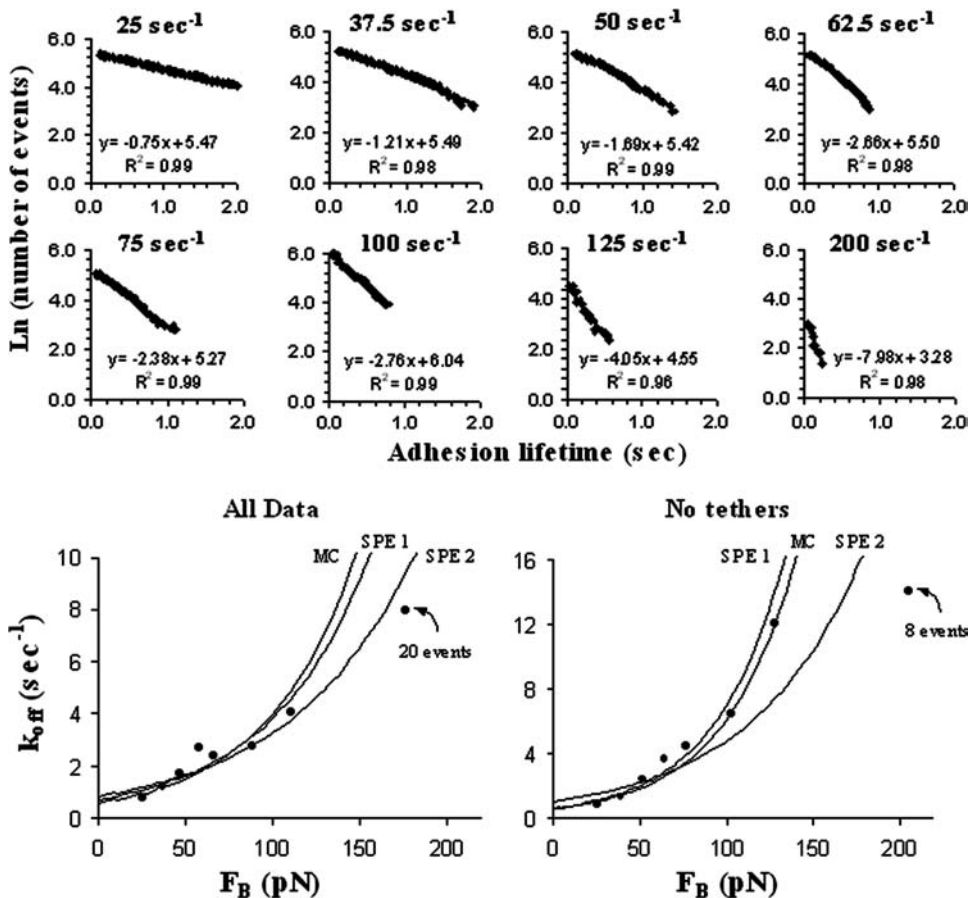


FIGURE 4 Kinetics of dissociation for the P-selectin/PSGL-1 bond. The linear fit of the curve through $\ln(N)$ versus t , where N is the number of events lasting at least t s, yields a slope of $-k_{\text{off}}$. Presented are the slopes $-k_{\text{off}}$ for all data (\pm tethers) at all shear rates (A). Values for k_{off} obtained in this manner were used to determine the unloaded off-rate $k_{\text{off}}(0)$ and reactive compliance, r , by determining a least-squares fit of an exponential curve through the plot of k_{off} versus F_B for all data (\pm tethers) (B) and interactions without membrane tether formation (C). Because the data at $\gamma_w = 200 \text{ s}^{-1}$ was sparse and appeared to be an outlier when compared with a global Monte Carlo simulation of collisions at all shear rates (MC in B and C), we regressed the plot including (SPE 2) or neglecting (SPE 1) k_{off} at 200 s^{-1} .

unusual teardrop shape (Fig. 1 *F*). This effect was not observed with any of the other treatments.

None of the treatments significantly altered the primary capture efficiency of the neutrophils with the P-selectin-coated bead (Fig. 6 *A*), indicating that the reagents had minimal effect on the concentration or activity of PSGL-1 on the neutrophil surface. Only latrunculin treatment caused a slight increase in the fraction of cells that formed membrane tethers ($p = 0.024$; Fig. 6 *B*) due to the extreme softness of the cells. Cytochalasin D and jasplakinolide had no significant effect on the membrane tether formation fraction. Cholesterol-depleting M β CD significantly reduced the likelihood that cells would form membrane tethers at $\gamma_w = 100 \text{ s}^{-1}$ ($p = 0.0007$), as did fixation of the cells with formaldehyde ($p < 0.0001$). All of the treatments significantly altered the average membrane tether length pulled from the cell (Fig. 6 *C*), with actin-depolymerizing reagents associated with an overall increase in membrane tether length, and cholesterol depletion and fixation with decreased membrane tether lengths. Interestingly, jasplakinolide, which acts to polymerize actin in the cell, had an affect similar to the depolymerizing reagents—likely due to the membrane blebbing observed.

For all chemical treatments (excluding formaldehyde, where no tethers formed), the set of adhesion lifetimes with

membrane tether formation was significantly longer than the lifetime without tethers ($p < 0.0001$) (Fig. 6 *D*). All of the treatments caused a significant overall change in the adhesion lifetimes (Fig. 6 *E*), and latrunculin was the only reagent that hardly altered (14.6% prolongation, $p = 0.079$) the lifetimes of membrane-tether forming adhesions, potentially due to the distinct morphology of tethering involving the entire cell (Fig. 1 *F*). Too few membrane tethers were pulled from formaldehyde-treated cells to allow analysis ($n = 1$). Fixation and cholesterol depletion caused a general decrease in overall adhesion lifetime with treatment, whereas the actin-depolymerizing agents increased the lifetime of interactions. Similar to our results for the average tether length, jasplakinolide acted in a similar manner as the depolymerizing agents.

The tether growth rates (v_{tether}) for membrane-tether-forming interactions of treated neutrophils with P-selectin-coated beads were also analyzed (Fig. 7). These results were compared against the average tether growth rate for untreated cells perfused over beads at 100 s^{-1} (average $v_{\text{tether}} = 8.1 \pm 4.9 \mu\text{m/s}$), and Student's t -tests were performed comparing the set of control cell growth rates to those for the treated cells. In all cases except latrunculin (where cells had an unusual morphology), treatment with actin- or cholesterol-affecting reagents caused significant differences between the two

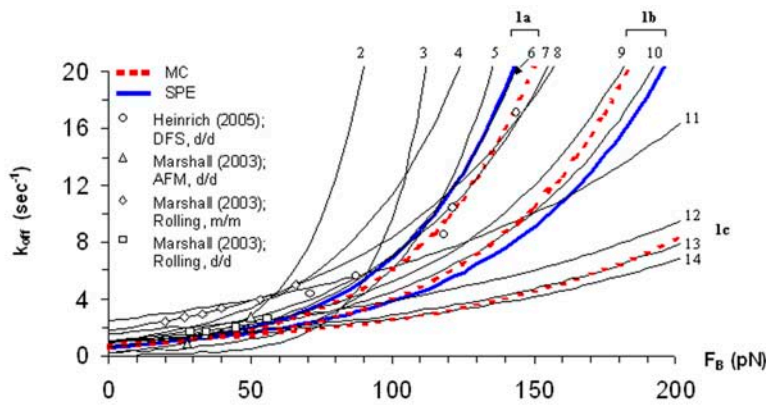


FIGURE 5 Bell model parameters for the PSGL-1/P-selectin bond. The Bell model parameters for the PSGL-1/P-selectin bond were compared against several previous studies (1–7,9,10,14,33) by fitting each with the Bell model and graphing k_{off} versus the force on the bond, F_B . Data of Heinrich et al. (Fig. 7 in (14)) was plotted (*top panel*) for $k_{\text{off}} = (\text{attachment lifetime})^{-1}$ as a function of F_{bond} where F_{bond} was set equal to f_{∞} (the nearly constant rupture force) calculated from the applied pulling rate (v_{pull} in $\mu\text{m/s}$) by $f_{\infty} = 60 \text{ pN}(v_{\text{pull}})^{0.25}$ that was used to generate the initial loading rate (r_f in pN/s , a value that rapidly plummets), thereby allowing a determination (*bottom panel*) of Bell parameters ($R^2 = 0.98$) for $71.4 < f_{\infty} < 210$ pN. (Nomenclature: *d/d*, dimeric PSGL-1/dimeric P-selectin interaction; *m/m*, monomeric PSGL-1/monomeric P-selectin interaction; *dPSGL1*, dimeric PSGL-1; *dP-selectin*, dimeric P-selectin; *SPE*, statistical point estimate; and *MC*, Monte Carlo simulation.)

Reference	$k_{\text{off}}(0)$ (sec^{-1})	r (nm)	Method
1a - Current study, w/o tethers	0.56	0.10	Bead collision - SPE
	0.53	0.10	Bead collision - MC ($n = 1$ bond)
1b - Current study, all data	0.67	0.07	Bead collision - SPE
	0.57	0.08	Bead collision - MC ($n = 1$ bond)
	0.53	0.10	Bead collision - MC ($n_{\text{avg}} = 1.48$ bonds)
1c - Apparent (for 0.53 sec^{-1}, 0.10 nm)	0.76	0.05	MC ($n = 2$ bonds)
2 - Marshall, et al, 2003	0.24	0.2	AFM w/o cells; dPSGL1/dP-selectin
3 - Fritz, et al, 1998	0.022	0.25	AFM w/o cells; dPSGL1/dP-selectin
4 - Yago, et al, 2002	1.0	0.10	Rolling beads; mPSGL1/mP-selectin
5 - Hanley, et al, 2003 and 2004	0.2	0.14	AFM w/cells; dPSGL1/dP-selectin
6 - Heinrich, et al, 2005	0.66	0.10	DFS; dPSGL1/dP-selectin
7 - Marshall, et al, 2003	1.78	0.06	Rolling beads; mPSGL1/mP-selectin
8 - Yago, et al, 2002	1.0	0.08	Rolling beads; dPSGL1/dP-selectin
9 - Marshall, et al, 2003	0.96	0.07	Rolling cells; dPSGL1/dP-selectin
10 - Chen and Springer, 2001	0.84	0.068	Rolling cells; dPSGL1/dP-selectin
11 - Smith, et al, 1999	2.4	0.039	Rolling cells; dPSGL1/dP-selectin
12 - Park, et al, 2002	1.54	0.037	Rolling beads/fixd cells; dPSGL1/dP-selectin
13 - Ramachandran, et al, 2001	1.0	0.042	Rolling cells; dPSGL1/dP-selectin
14 - Alon, et al, 1997	0.95	0.04	Rolling cells; dPSGL1/dP-selectin

samples. Cytochalasin and jasplakinolide both caused tethers to grow faster than untreated cells, whereas cholesterol depletion decreased the tether growth rate relative to untreated cells. In comparing the tether growth rate velocity for all events (*solid bar*, Fig. 7 A) with the measured lifetimes of those events (Fig. 6 E), it was clear that increases in the tether growth velocity caused prolongation in the PSGL-1/P-selectin lifetime due to decreased forces on the bonds (Fig. 7 B). It would be highly unlikely that the lifetime of the tether attachment to the bead would alter the tether growth rate velocity, a process that is dictated by lipid flow from the neutrophil.

DISCUSSION

Beads coated with P-selectin and adsorbed onto flow chamber surfaces served as discrete sources of ligand for studying the function of PSGL-1 in the native membrane of neutrophils. This new method allowed the simultaneous probing of several distinct processes in tether growth and P-selectin/PSGL-1 bond formation and rupture under hemodynamic venous flow conditions.

A central issue addressed by this technique was whether tether growth shields the bond from force loading, and to what extent. The data in Fig. 2 D comparing the average lifetime of populations with and without tethers at each shear rate suggests, but does not prove, that tether growth results in longer lived bonds. Long-lived bonds allow more time for tether growth and consequently longer tethers. Short-lived

bonds provide less time for tether growth and thus result in shorter tethers. We have used five different pharmacological treatments to alter membrane and cell mechanics. The most extreme treatment was formaldehyde fixation, which obliterated tether formation and reduced the bond lifetime to a level identical to that found for events that did not form tethers using unfixed neutrophils (Fig. 6 D). Since the collision efficiency was not reduced with formaldehyde, this reduction in the overall lifetime of all events by formaldehyde was not likely due to a defect in the bond or the level of PSGL-1 on the fixed neutrophil. This result extends the prior understanding of formaldehyde effects (3) by simultaneously measuring both tether length and bond life for each adhesion event. A less extreme method of reducing tether growth was achieved through the use of $M\beta\text{CD}$ to extract cholesterol out of the neutrophil membrane. $M\beta\text{CD}$ reduced the fraction of cells forming tethers and reduced the tether length and the tether growth velocity, but not to the extent achieved with formaldehyde. Consistent with tether length shielding the bond from loading, $M\beta\text{CD}$ reduced the overall lifetime of bonds. Since the collision efficiency was not reduced with $M\beta\text{CD}$, this reduction in the overall lifetime of all events by $M\beta\text{CD}$ was not likely due to a defect in the bond or the level of PSGL-1 on the surface of cholesterol-depleted neutrophils. $M\beta\text{CD}$ has previously been reported to increase leukocyte rolling velocity (33). On a local scale of the plasmalemma at the base of the tether, neutrophils depleted of cholesterol exhibit the rigidifying effects that have

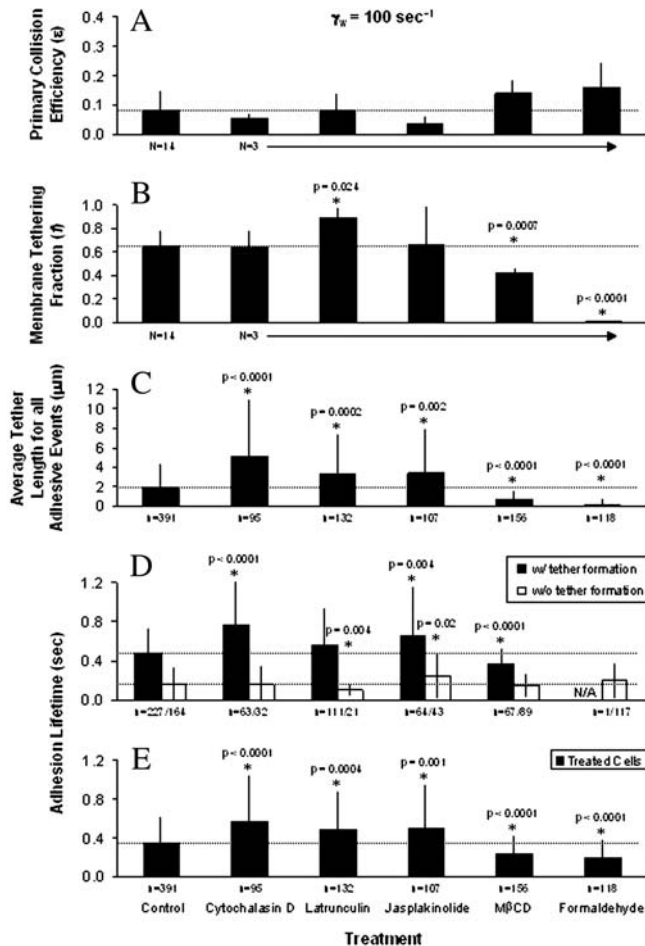


FIGURE 6 Adhesion dynamics for chemically treated neutrophils. The average primary adhesion collision efficiencies ϵ (A) and the membrane tethering fractions f (B) between treated neutrophils and selectin-coated beads were calculated over N donors. Membrane tether lengths were measured and averaged for all neutrophils making adhesive collisions (C), and the average lifetimes for all the adhesive and nonadhesive events were also calculated (E). The lifetimes were then binned according to whether discernible membrane tethers were formed (D). Error bars refer to standard deviations for N donors or n collisions.

previously been demonstrated on a global whole-cell scale using micropipette aspiration (33).

Conversely, agents that caused longer tethers to form (cytochalasin D, latrunculin, and jasplakinolide) also prolonged the average lifetime of the adhesive interaction (Fig. 6 D). Latrunculin softens the entire cell body and causes an unusual tear-shape morphology in the bead collision assay, which may lead to cell flattening and reduction of force loading at a given shear rate. In contrast, jasplakinolide hardens the overall cell but causes plasmalemma blebbing, which in turn facilitates membrane tether formation (an increase in f) because lipid is already detached from the cytoskeleton and available for flow into the tether. Jasplakinolide serves as an example where whole cell mechanics, i.e., cell hardening as detected by micropipette aspiration (37), does not predict local plasmalemma dynamics during PSGL-1-mediated

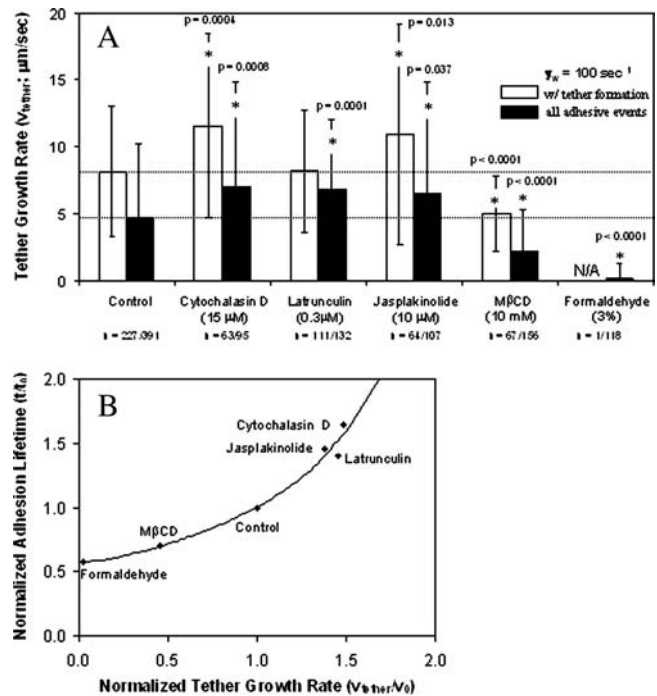


FIGURE 7 Tether growth rates for neutrophils under several conditions. Tether growth rates were calculated for neutrophils treated with membrane or cytoskeleton altering reagents, and perfused over selectin-coated beads at $\gamma_w = 100 \text{ s}^{-1}$. Tether growth rates were calculated based on averages over all adhesive events (solid bars in A), and also specifically for membrane-tether-forming events (open bars in A). These results were compared versus untreated data at the same shear rate (A). Stars represent data for which the treated data set was significantly different ($p < 0.05$) than control data. Results returned from a two-tailed Student's t -test are shown for all data that differed significantly from control. Averages are for $n > 60$ collisions and $N \geq 3$ donors, and error bars given are for standard deviation. Tether growth rates for treated neutrophils (v_{tether}) were then normalized by the tether growth rate of untreated cells at the same wall shear rate (v_0). These were then compared to normalized adhesion lifetimes (t/t_0) for all adhesive events (B).

bonding. In the study of Sheikh et al. (37), it was only the neutrophil core that would resist entry into the pipette; membrane blebs that had formed on the surface of the cells would easily enter. We also observed membrane blebs on the surface of neutrophils treated with this reagent (not shown), which indicated that the lipid bilayer separated from the neutrophil at these locations (51). This separation of bilayer and cytoskeleton reduces the minimum force necessary to pull a tether by eliminating the membrane-cytoskeletal adhesion portion of tether adhesion energy (51), thus rendering the cell locally as less rigid than untreated cells.

Micropipette studies looking at global effects on rigidity due to cytochalasin D (32–34) through measurement of the cortical viscosity previously pointed to depolymerization as a mechanism of neutrophil softening. Other studies looking specifically at tether growth after treatment with either cytochalasin D (23) or latrunculin A (36) have shown that the membrane slip between the lipid bilayer and cytoskeleton is a major contributor to energy dissipation during tether

formation. In our study, on average, membrane tethers generated by cells treated with cytochalasin D or latrunculin A had faster tether growth rates (Fig. 7) than untreated cells, and consequently longer bond lifetimes than untreated cells (Fig. 6). These results point to a greater ease of lipid flow into the tether during formation under venous flow conditions. Neutrophils that were fixed or treated with M β CD had opposite effects to those seen with depolymerizing agents, and formed tethers with significantly reduced growth rates compared to untreated cells and consequently had shorter lifetimes (Figs. 6 and 7). A force as low as 25.6 pN at a wall shear rate of 25 s⁻¹ was detected to cause membrane tether pulling. This force is ~50% of that predicted by micropipette studies, where micromanipulation of the cell may lead to low level cellular activation and consequent slight cortical stiffening.

Since this study focused on both on-rate and off-rate processes, a high saturating level of P-selectin IgG chimera was used in these studies to allow a reliable determination of the collision efficiency as a function of shear rate (Fig. 2 A). Since the contact area is so small at the tip of the tether and the interaction time so short during the actual neutrophil-bead collision (Fig. 2 E), the method resulted in events dominated by single bond interactions (estimated at >65%) and provided Bell parameters that were consistent with those obtained from rolling experiments (curve 1b in Fig. 5). A subset of all events, those without tethers where forces are most uniform and accurately estimated at each γ_w (curve 1a in Fig. 4 B), provided Bell parameters consistent with single-bond MC and prior AFM and rolling beads experiments (curves 2–8 in Fig. 5). Rebonding processes (k_{on} in the MC) did not appear significant in the data sets and this suggests that the contact area at the tip of the tether, when pulled, becomes exceedingly small, possibly approaching the dimensions of an AFM cantilever tip. Future work employing sparsely-coated beads that is focused solely on off-processes (where ϵ is not determined) should allow the event distribution to be dominated by single bonds.

Catch-bonding has been detected by AFM and in flow chambers for the PSGL-1/P-selectin bond at force loadings in the 5–20 pN range (7). Catch-bonding may be one of several underlying mechanisms to explain the unexpected hydrodynamic-thresholding observed for neutrophil rolling on selectins (35). Platelet translocation on vWF A1 domain also displays thresholding at ~1 dyn/cm² (44) with $r > 0$ at $F_{bond} > 36$ pN. Neutrophils rolling on selectin-coated surfaces display biphasic force-enhanced adhesion at low shears, and force-decreased adhesion at shear rates above a certain maximum in shear (52). The direct observation of a decrease in off-rate at low shear rates that switches to an increase at higher shear rates provided the first experimental observation of catch-bonding in the P-selectin/PSGL-1 system (7). Catch-bonding has also been reported for L-selectin/PSGL-1 at low forces (8,53). In the current study, we did not look at the force regime below the catch-bond

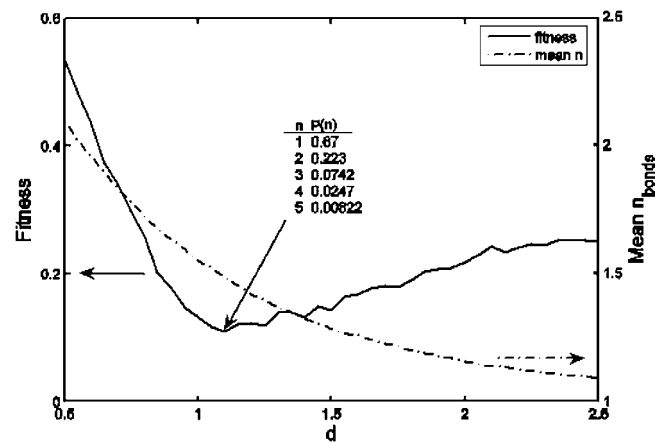


FIGURE A1 Dependence on number of bonds. The number of initial bonds present affects the simulation because of the division of forces between them. The distribution weighting factor (d) describes how the initial number of bonds were allocated according to the exponential probability of $\exp(-dn)$ for $n = 1-5$. These distribution weighting factors indicate the best fit at $d = 1.1$ (solid line, left scale) with a mean number of bonds of 1.48 (dashed line, right scale). The Bell parameters used were $k_{on} = 0$ s⁻¹, $k_{off}^0 = 0.53$ s⁻¹, and $r = 0.10$ nm. Two-thousand simulations were averaged at each data point shown.

threshold for P-selectin/PSGL-1 ($F_B < 10-20$ pN, $\gamma_w < 15$ s⁻¹), and thus our results are for those interactions in the slip-bond regime only.

The neutrophil-bead collision assay may prove useful in future studies, including: determination of the on-rate as a function of shear rate and ligand density; thresholding studies at low flows where contaminating flow fluctuations would have to be coincident with the bead collision and thus hydrodynamic fluctuation effects are better filtered out of the assay; studies of activated neutrophils to probe VCAM-1 or ICAM-1 binding lifetimes; or the analysis of patient neutrophils where neutrophil membrane mechanics and inflammation are potential cofactors in vaso-occlusive phenomena.

APPENDIX

For the distribution of initial bond studies, 2000 simulations were run with distribution weighting factors between 0.5 and 2.5 (Fig. A1). The best fit indicated an exponential distribution constant of $d = 1.1$, causing a mean initial number of bonds of 1.48; however, the minimum is shallow and jagged, so the true minimum may be between $d = 1.1$ and 1.5 (1.28 and 1.55 mean initial bonds), with ~65–75% of the tethers having only a single bond present.

Authors acknowledge helpful conversations with Dr. M. B. Lawrence (University of Virginia).

This work was supported by National Institutes of Health grant No. HL56621 (to S.L.D.). K.E.E. is a recipient of an Ashton Fellowship.

REFERENCES

- Alon, R., S. Chen, K. D. Puri, E. B. Finger, and T. A. Springer. 1997. The kinetics of L-selectin tethers and the mechanics of selectin-mediated rolling. *J. Cell Biol.* 138:1169–1180.

2. Chen, S., and T. A. Springer. 2001. Selectin receptor-ligand bonds: Formation limited by shear rate and dissociation governed by the Bell model. *Proc. Natl. Acad. Sci. USA*. 98:950–955.
3. Park, E. Y. H., M. J. Smith, E. S. Stropp, K. R. Snapp, J. A. DiVietro, W. F. Walker, D. W. Schmidtke, S. L. Diamond, and M. B. Lawrence. 2002. Comparison of PSGL-1 microbead and neutrophil rolling: microvillus elongation stabilizes P-selectin bond clusters. *Biophys. J.* 82:1835–1847.
4. Ramachandran, V., T. Yago, T. K. Epperson, M. M. A. Kobzdej, M. U. Nollert, R. D. Cummings, C. Zhu, and R. P. McEver. 2001. Dimerization of a selectin and its ligand stabilizes cell rolling and enhances tether strength in shear flow. *Proc. Natl. Acad. Sci. USA*. 98:10166–10171.
5. Smith, M. J., E. L. Berg, and M. B. Lawrence. 1999. A direct comparison of selectin-mediated transient, adhesive events using high temporal resolution. *Biophys. J.* 77:3371–3383.
6. Fritz, J., A. G. Katopodis, F. Kolbinger, and D. Anselmetti. 1998. Force-mediated kinetics of single P-selectin/ligand complexes observed by atomic force microscopy. *Proc. Natl. Acad. Sci. USA*. 95:12283–12288.
7. Marshall, B. T., M. Long, J. W. Piper, T. Yago, R. P. McEver, and C. Zhu. 2003. Direct observation of catch bonds involving cell-adhesion molecules. *Nature*. 423:190–193.
8. Sarangapani, K. K., T. Yago, A. G. Klopocki, M. B. Lawrence, C. B. Fieger, S. D. Rosen, R. P. McEver, and C. Zhu. 2004. Low force decelerates L-selectin dissociation from P-selectin glycoprotein ligand-1 and endoglycan. *J. Biol. Chem.* 279:2291–2298.
9. Hanley, W., O. McCarty, S. Jadhav, Y. Tseng, D. Wirtz, and K. Konstantopoulos. 2003. Single molecule characterization of P-selectin/ligand binding. *J. Biol. Chem.* 278:10556–10561.
10. Hanley, W., D. Wirtz, and K. Konstantopoulos. 2004. Distinct kinetic and mechanical properties govern selectin-leukocyte interactions. *J. Cell Sci.* 117:2503–2511.
11. Rinko, L. J., M. B. Lawrence, and W. H. Guilford. 2004. The molecular mechanics of P- and L-selectin lectin domains binding to PSGL-1. *Biophys. J.* 86:544–554.
12. Evans, E., A. Leung, D. Hammer, and S. Simon. 2001. Chemically distinct transition states govern rapid dissociation of single L-selectin bonds under force. *Proc. Natl. Acad. Sci. USA*. 98:3784–3789.
13. Evans, E., A. Leung, V. Heinrich, and C. Zhu. 2004. Mechanical switching and coupling between two dissociation pathways in a P-selectin adhesion bond. *Proc. Natl. Acad. Sci. USA*. 101:11281–11286.
14. Heinrich, V., A. Leung, and E. Evans. 2005. Nano- to microscale dynamics of P-selectin detachment from leukocyte interfaces. II. Tether flow terminated by P-selectin dissociation from PSGL-1. *Biophys. J.* 88:2299–2308.
15. Mehta, P., R. D. Cummings, and R. P. McEver. 1998. Affinity and kinetic analysis of P-selectin binding to P-selectin glycoprotein ligand-1. *J. Biol. Chem.* 273:32506–32513.
16. Marshall, B. T., K. K. Sarangapani, J. Lou, R. P. McEver, and C. Zhu. 2005. Force history dependence of receptor-ligand dissociation. *Biophys. J.* 88:1458–1466.
17. Shao, J. Y., H. P. Ting-Beall, and R. M. Hochmuth. 1998. Static and dynamic lengths of neutrophil microvilli. *Proc. Natl. Acad. Sci. USA*. 95:6797–6802.
18. Schmidtke, D. W., and S. L. Diamond. 2000. Direct observation of membrane tethers formed during neutrophil attachment to platelets or P-selectin under physiological flow. *J. Cell Biol.* 149:719–729.
19. Evans, E., V. Heinrich, A. Leung, and K. Kinoshita. 2005. Nano- to microscale dynamics of P-selectin detachment from leukocyte interfaces. I. Membrane separation from the cytoskeleton. *Biophys. J.* 88:2288–2298.
20. Zhu, C., M. Long, S. E. Chesla, and P. Bongrand. 2002. Measuring receptor/ligand interaction at the single-bond level: experimental and interpretive issues. *Ann. Biomed. Eng.* 30:305–314.
21. Puri, K. D., E. B. Finger, and T. A. Springer. 1997. The faster rolling kinetics of L-selectin than E-selectin and P-selectin rolling at comparable binding strength. *J. Immunol.* 158:405–413.
22. Shao, J. Y., and R. M. Hochmuth. 1996. Micropipette suction for measuring piconewton forces of adhesion and tether formation from neutrophil membranes. *Biophys. J.* 71:2892–2901.
23. Shao, J. Y., and J. Xu. 2002. A modified micropipette aspiration technique and its application to tether formation from human neutrophils. *J. Biomech. Eng. Trans. ASME*. 124:388–396.
24. Girdhar, G., and J. Y. Shao. 2004. Membrane tether extraction from human umbilical vein endothelial cells and its implication in leukocyte rolling. *Biophys. J.* 87:3561–3568.
25. Spector, I., F. Braet, N. R. Shochet, and M. R. Bubb. 1999. New anti-actin drugs in the study of the organization and function of the actin cytoskeleton. *Microsc. Res. Tech.* 47:18–37.
26. Torres, M., and T. D. Coates. 1999. Function of the cytoskeleton in human neutrophils and methods for evaluation. *J. Immunol. Methods*. 232:89–109.
27. McCarty, O. J. T., N. Tien, B. S. Bochner, and K. Konstantopoulos. 2003. Exogenous eosinophil activation converts PSGL-1-dependent binding to CD18-dependent stable adhesion to platelets in shear flow. *Am. J. Physiol. Cell Physiol.* 284:C1223–C1234.
28. Bubb, M. R., A. M. J. Senderowicz, E. A. Sausville, K. L. K. Duncan, and E. D. Korn. 1994. Jaspilakinolide, a cytotoxic natural product, induces actin polymerization and competitively inhibits the binding of phalloidin to F-actin. *J. Biol. Chem.* 269:14869–14871.
29. Bubb, M. R., I. Spector, B. B. Beyer, and K. M. Fosen. 2000. Effects of jaspilakinolide on the kinetics of actin polymerization. *J. Biol. Chem.* 275:5163–5170.
30. Senderowicz, A. M., G. Kaurm, E. Sainz, C. Laing, W. D. Inman, J. Rodriguez, P. Crews, L. Malspeis, M. R. Grever, and E. A. Sausville. 1995. Jaspilakinolide's inhibition of the growth of prostate carcinoma cells in vitro with disruption of the actin cytoskeleton. *J. Nat. Can. Inst.* 87:46–51.
31. Tsai, M. A., R. S. Frank, and R. E. Waugh. 1994. Passive mechanical behavior of human neutrophils: effect of cytochalasin B. *Biophys. J.* 66:2166–2172.
32. Ting-Beall, H. P., A. S. Lee, and R. M. Hochmuth. 1995. Effect of cytochalasin D on the mechanical properties and morphology of passive human neutrophils. *Ann. Biomed. Eng.* 23:666–671.
33. Yago, T., A. Leppanen, H. Qiu, W. D. Marcus, M. U. Nollert, C. Zhu, R. D. Cummings, and R. P. McEver. 2002. Distinct molecular and cellular contributions to stabilizing selectin-mediated rolling under flow. *J. Cell Biol.* 4:787–799.
34. Sheikh, S., and G. B. Nash. 1998. Treatment of neutrophils with cytochalasins converts rolling to stationary adhesion on P-selectin. *J. Cell. Physiol.* 174:206–216.
35. Finger, E. B., R. E. Bruehl, D. F. Bainton, and T. A. Springer. 1996. A differential role for cell shape in neutrophil tethering and rolling on endothelial selectins under flow. *J. Immunol.* 157:5085–5096.
36. Marcus, W. D., and R. M. Hochmuth. 2002. Experimental studies of membrane tethers formed from human neutrophils. *Ann. Biomed. Eng.* 30:1273–1280.
37. Sheikh, S., W. B. Gratzer, J. C. Pinder, and G. B. Nash. 1997. Actin polymerization regulates integrin-mediated adhesion as well as rigidity of neutrophils. *Biochem. Biophys. Res. Commun.* 238:910–915.
38. Rotsch, C., and M. Radmacher. 2000. Drug-induced changes of cytoskeletal structure and mechanics in fibroblasts: an atomic force microscopy study. *Biophys. J.* 78:520–535.
39. Christian, A. E., M. P. Haynes, M. C. Phillips, and G. H. Rothblat. 1997. Use of cyclodextrins for manipulating cellular cholesterol content. *J. Lipid Res.* 38:2264–2272.
40. Pierini, L. M., R. J. Eddy, M. Fuortes, S. Seveau, C. Casulo, and F. R. Maxfield. 2003. *J. Biol. Chem.* 278:10831–10841.

41. Goel, M. S., and S. L. Diamond. 2001. Neutrophil enhancement of fibrin deposition under flow through platelet-dependent and -independent mechanisms. *Arterioscler. Thromb. Vasc. Biol.* 12:2093–2098.
42. Rodgers, S. D., R. T. Camphausen, and D. A. Hammer. 2000. Sialyl Lewis x-mediated, PSGL-1-independent rolling adhesion of P-selectin. *Biophys. J.* 79:694–706.
43. Goldman, A. J., R. G. Cox, and H. Brenner. 1967. Slow viscous motion of a sphere parallel to a plane wall. II. Couette flow. *Chem. Eng. Sci.* 22:653–660.
44. Doggett, T. A., G. Girdhar, A. Lawshe, D. W. Schmidtke, I. J. Laurenzi, S. L. Diamond, and T. G. Diacovo. 2002. Selectin-like kinetics and biomechanics promote rapid platelet adhesion in flow: the GPIIb- α -vWF-tether bond. *Biophys. J.* 83:194–205.
45. Gillespie, D. T. 1977. Exact stochastic simulation of coupled chemical reactions. *J. Phys. Chem.* 81:2340–2361.
46. Hochmuth, R. M., and W. D. Marcus. 2002. Membrane tethers formed from blood cells with available area and determination of their adhesion energy. *Biophys. J.* 82:2964–2969.
47. Moore, K. L., K. D. Patel, R. E. Bruehl, F. Li, D. A. Johnson, H. S. Lichenstein, R. D. Cummings, D. F. Bainton, and R. P. McEver. 1995. P-selectin glycoprotein ligand-1 mediates rolling of human neutrophils on P-selectin. *J. Cell Biol.* 128:661–671.
48. Jadhav, S., C. D. Eggleton, and K. Konstantopoulos. 2005. A 3-D computational model predicts that cell deformation affects selectin-mediated leukocyte rolling. *Biophys. J.* 88:96–104.
49. Chen, S., and T. A. Springer. 1999. An automatic braking system that stabilizes leukocyte rolling by an increase in selectin bond number with shear. *J. Cell Biol.* 144:185–200.
50. King, M. R., V. Heinrich, E. Evans, and D. A. Hammer. 2005. Nano-to-microscale dynamics of P-selectin detachment from leukocyte interfaces. III. Numerical simulation of tethering under flow. *Biophys. J.* 88:1676–1683.
51. Dai, J., and M. P. Sheetz. 1999. Membrane tether formation from blebbing cells. *Biophys. J.* 77:3363–3370.
52. Konstantopoulos, K., W. D. Hanley, and D. Wirtz. 2003. Receptor-ligand binding: “catch” bonds finally caught. *Curr. Biol.* 13:R611–R613.
53. Yago, T., J. Wu, C. D. Wey, A. G. Klopocki, C. Zhu, and R. P. McEver. 2004. Catch bonds govern adhesion through L-selectin at threshold shear. *J. Cell Biol.* 166:913–923.